PROF. JOHN BOULOS (Orcid ID : 0000-0001-8561-6418)

Article type : Research Article

TITLE PAGE

TITLE

SYNTHESIS OF NOVEL AND FUNCTIONALLY SELECTIVE NON-COMPETITIVE MUSCARINIC ANTAGONISTS AS CHEMICAL PROBES

SHORT TITLE

Muscarinic Antagonists as probes

KEY WORDS

PD- Parkinson Disease

GPCR- G-Protein-coupled receptor

mAChR- Muscarinic acetylcholine receptor

PAM- Positive allosteric modulator

NMS- N-methylscopolamine

AUTHORS

John F. Boulos, Department of Physical Sciences, Barry University, Miami Shores, Florida 33161,

Tel. 305-899-3432, Fax 305-899-3479, email: jboulos@barry.edu

This article has been accepted for publication and undergone full peer review but has not been through the copyediting, typesetting, pagination and proofreading process, which may lead to differences between this version and the Version of Record. Please cite this article as doi: 10.1111/cbdd.13059

CO-AUTHORS

Jan Jakubik, Department of Neurochemistry, Institute of Physiology of the Academy of Sciences of the Czech Republic, v.v.i., 142 20 Prague, Czech Republic, Tel. +420 2 4106 2620, Fax +420 2 4106 2488, email: jan.jakubik@fgu.cas.cz

John M. Boulos, University of North Carolina, Eshelman School of Pharmacy, Chapel Hill, North Carolina, 27559, Tel. 305-332-7232, email: jmboulos12@gmail.com

Alena Randakova, Department of Neurochemistry, Institute of Physiology of the Academy of Sciences of the Czech Republic, v.v.i., 142 20 Prague, Czech Republic, Tel. +420 2 4106 2620, Fax +420 2 4106 2488,

Alena.randakova@fgu.cas.cz

Jelena Momirov, Department of Physical Sciences, Barry University, Miami Shores, Florida 33161, Tel. 305-899-3432, Fax 305-899-3479, email: Jelena.momirov@mymail.barry.edu

SYNTHESIS OF NOVEL AND FUNCTIONALLY SELECTIVE NON-COMPETITIVE MUSCARINIC ANTAGONISTS AS CHEMICAL PROBES

John F. Boulos, Jan Jakubik, John M. Boulos, Jelena Momirov, Alena Randakova

ABSTRACT: Muscarinic receptors are known to play important biological roles and are drug targets for several human diseases. In a pilot study, novel muscarinic antagonists were synthesized and used as chemical probes to obtain additional information of the muscarinic pharmacophore. The design of these ligands made use of current orthosteric and allosteric models of drug-receptor interactions together with chemical motifs known to achieve muscarinic receptor selectivity. This approach has led to the discovery of several non-competitive muscarinic ligands that strongly bind at a secondary

receptor site. These compounds were found to be non-competitive antagonists that completely abolished carbachol activation in functional assays. Several of these compounds antagonized functional response to carbachol with great potency at M_1 and M_4 than at the rest of receptor subtypes.

INTRODUCTION

Muscarinic receptor subtypes provide effective therapeutic targets for a number of neurological and psychiatric diseases such as Alzheimer's (AD), Schizophrenia (Sc) and Parkinson (PD). [1-3] Considerable biochemical and pharmacological evidence have validated the cholinergic hypothesis of memory dysfunction and led to the development of numerous selective allosteric and orthosteric muscarinic ligands. One such ligand, Xanomeline (**1**), M_1/M_4- functionally selective agonist, demonstrated beneficiary effects on cognitive decline in several AD patients and a similar therapeutic profile to antipsychotics drugs such as clozapine and olanzapine. [4-6]

Classical approaches to G-protein coupled receptor (GPCR) drug design have targeted the orthosteric receptor binding site and most drugs are known to interact with this endogenous ligand-binding pocket. Orthosteric ligands must overcome many limitations which make the development of subtype-specific agonists and antagonists very difficult. [7] Some G-protein coupled receptors (including muscarinic receptors) also contain less conserved allosteric binding sites that are targeted to attain receptor selectivity and to elicit distinct signaling profiles. Allosteric ligands exert their effects by modulating the binding affinity and downstream efficacy of the orthosterically bound ligand. [8] The use of allosteric muscarinic ligands, gallamine and alcuronium, in site-directed mutagenesis studies provided evidence for the "common" allosteric site. [9] The existence of a second allosteric site was proposed when indolocarbazole (KT5720) was found to allosterically enhance the binding of acetylcholine and N-methylscopolamine (NMS) at the M_1-M_4 receptors. [10] Numerous selective muscarinic ligands have been identified, including positive allosteric modulators (PAMs) and putative bitopic agonists. Benzyl quinolone carboxylic (BQCA, **2**) was the first M_1 muscarinic allosteric ligand

exhibiting absolute subtype selectivity and high degree of cooperativity. [11] Several allosteric modulators including heptane-1,7-bis(dimethyl-3'-phthalimidopropyl) ammonium bromide (C7/3-phth), gallamine and alcuronium were found to form cation-π interactions with the "common site" of the M_2 receptor. [12] These findings provide a structural basis for the rational design of allosteric modulators. The recent publications of crystallographic structures of muscarinic receptors will mostly help with the determination of actual binding sites and specific drug-receptor interactions. [13-15]

There exists substantial evidence for bitopic ligands, molecules that simultaneously bind to both the allosteric and orthosteric sites. [16-17] Xanomeline was shown to bind to the receptor in a wash-resistant manner, suggesting that it acts both competitively as well as allosterically. [18] Pharmacological studies revealed that compound AC-42 (**3***)*, a M_1-selective agonist, exhibits characteristics suggestive of both allosteric and orthosteric modes of action. [19] The potential of linking orthosteric and allosteric pharmacophores to yield bitopic ligands may lead to novel compounds with high potency and receptor selectivity that can elicit distinct signaling profiles.

We have synthesized and tested muscarinic ligands with the general formula **4** and structural features similar to both known agonists **1** and **3**. Several of these compounds were found to be functionally selective non-competitive antagonists. Compounds contain a para-disubstituted alkyl or alkoxy (R_1) phenyl group linked to a tetrahydropyridinyl ring. From measured radioligand binding and functional data, we concluded that the positively charged, tetrahydropyridinyl group, most likely interacts with the orthosteric receptor site whereas the hydrophobic phenyl moiety interacts more strongly with the secondary receptor site.

Compounds **9b** (R_1= n-C_4H_9, R_2= H), **10a** (R_1= O-n-C_4H_9, R_2= Me) and **10b** (R_1= n-C_4H_9, R_2= Me) (**scheme 1**) were found to be non-competitive M_1/M_4 functionally selective antagonists. These compounds antagonized response to carbachol at M_1 and M_4 receptors better than at other subtypes. Other compounds **5** of similar structural features, with a substituted piperidinyl ring, were also synthesized and found to exhibit similar biological profiles. The bitopic antagonist **13a** (**scheme 2**), our lead compound which led to the synthesis of all other analogs was found to slow down the

dissociation of both N-methyl scopolamine (NMS) and acetylcholine to the extent comparable to classical allosteric modulators gallamine and alcuronium at M_1-M_5 muscarinic receptors. [20] We plan on synthesizing other structural analogs with alkyl and alkoxy groups at both ortho and meta positions and others with an ether moiety, in place of the ester, to fully explore the large body of available information.

M_1 receptors were found to participate in the overall regulation of basal ganglia function and antiparkinsonian effects of muscarinic antagonists. [21] The competitive orthosteric M_1 selective antagonist VU0255035 was found to inhibit induction of generalized seizures by the agonist pilocarpine without the cognitive impairing effects of the antagonist scopolamine. [22] M_4 muscarinic receptors, expressed in different regions of the forebrain and co-expressed with D1 dopamine receptors, were found to play a critical role in modulating dopamine-dependent activities. [23] Based on those observations, we believe that our more functionally selective M_1/M_4 analogs may provide a viable approach for the treatment of certain central nervous system disorders including Parkinson (PD). [3] However, muscarinic antagonists may have somewhat limited clinical applications due to central and peripheral adverse effects.

METHODS AND MATERIALS

General Information

Reagents were purchased from Aldrich Chemical Company (St. Louis, MO) unless otherwise noted, and all starting liquid materials were distilled before use. NMR spectra were recorded on a Varian 300 MHz spectrometer. GC-MS spectra were recorded on a Perkin Elmer Clarus 500 and 560S system. Elemental analyses were carried out by Galbraith Laboratories (Knoxville, TN) and biological assays were conducted at the Institute of Physiology of the Czech Academy of Sciences in Prague. Melting points were recorded on a Digimelt MPA160 purchased from Stanford Research Systems and are uncorrected. Refractive indexes were recorded on r^2 i300 digital refractometer from Reichert Technologies corrected for 20 ^oC. The radioligands [^{3}H]-N-methylscopolamine chloride ([^{3}H]-NMS),

and [^{3}H]-myo-inositol were purchased from American Radiolabeled Chemicals (St. Louis, MO, USA). Carbachol, dithiothreitol, ethylendiaminotetraacetic acid (EDTA), and N-methylscopolamine chloride (NMS) were purchased from Sigma (St. Louis, MO, USA).

Synthesis

1-(2-hydroxyethyl) pyridinium bromide (6) A solution of 10.07 g of 2-bromoethanol (0.0805 mol) in 20 mL of acetonitrile was added slowly to another solution containing 6.36 g of pyridine (0.0804 mol) and 20 mL of acetonitrile. After addition, the mixture was allowed to stir for 6 days and then refluxed for one hour. The mixture was then concentrated and residue recrystallized from n-butanol to yield 11.79 g (72.3%) of white crystals, m.p. 102.5-103.0 ^{o}C. ^{1}H-NMR (D_2O): δ 8.75 (2H, d), 8.45 (1H, t), 7.95 (2H, t), 4.6 (2H, t), 3.9 (2H, t). MS (m/z): 79.01 base $[C_5H_5N]^+$.

1-(2-hydroxyethyl)-1,2,5,6-tetrahydropyridine (7) To a mixture containing 7.10 g of **6** (0.0348 mol) and 100 mL of methanol, a solution of sodium borohydride (5.25 g, 0.139 mol) in 60 mL of 0.1 M sodium hydroxide was added slowly with external cooling (ice-bath). The mixture was then allowed to stir at room temperature for an additional 30 minutes. 6 M hydrochloric acid was added to pH 5 and the solution was then brought to pH 8 with 3 M of sodium hydroxide. The mixture was extracted with dichloromethane, dried over anhydrous magnesium sulfate and concentrated to yield 1.24 g (28.0%). ^{1}H-NMR (CD_3COCD_3): δ5.75 (1H, m), 5.65 (1H, m), 4.0-4.2 (1H,bs), 3.7 (2H, t), 3.05 (2H, t), 2.65 (4H, m), 2.15 (2H, m). MS (m/z): M^+ 127.08, 96.03 base $[C_6H_{10}N]^+$, 82.00 $[C_5H_8N]^+$.

2-(1,2,5,6-tetrahydropyridine-N-ethyl)-4-butoxybenzoate 8(a) 2.07 g of 4-butoxy benzoylchloride (0.00974 mol) in 5 mL of diethyl ether was added slowly to a solution of **7** (1.24 g, 0.00974 mol) in 10 mL of anhydrous ether and 1.0 gram (0.0094 mol) of sodium carbonate. The mixture was stirred at room temperature for one hour. Diethyl ether was added and the excess carbonate was filtered off. The filtrate was adjusted to pH 8 with 6M sodium hydroxide and the mixture extracted with ether. Combined ether extracts was dried over magnesium sulfate and concentrated to afford 1.84 g (62.4%). ^{1}H-NMR ($CDCl_3$): δ 7.9 (2H, d), 6.9 (2H, d), 6.9 (1H, m), 6.7 (1H, m), 4.7 (2H, t), 4.0 (2H, t), 3.5 (2H, t), 3.2 (2H, d), 3.1 (2H, t), 2.4 (2H, m), 1.8 (2H, m), 1.5 (2H, m), 1.0 (3H, t). MS (m/z): M^+

303.18, 96.05 base $[C_6H_{10}N]^+$,109.05 $[C_7H_{11}N]^+$, 82.00 $[C_5H_8N]^+$.

2-(1,2,5,6-tetrahydropyridine-N-ethyl)-4-butoxybenzoate hydrochloride 9(a) Hydrogen chloride gas was bubbled through a solution containing 0.50 g (0.00165 mol) of **8a** and 5 mL of acetonitrile. The solution was concentrated to afford 0.55 g of a solid residue. The solid was recrystallized from n-butanol to yield 0.42 g (75.0%), m.p. 145-147 °C. ^{1}H-NMR (D_2O): δ 7.8 (2H, d), 6.9 (2H, d), 5.8 (1H, m), 5.5 (1H, m), 4.5 (2H, t), 3.9 (2H, d), 3.7 (2H, t), 3.5 (2H, t), 3.3 (2H, t), 2.3 (2H, m), 1.6 (2H, m), 1.3 (2H, m), 0.7 (3H, t). Elemental analysis calculated (%) for $C_{18}H_{26}NO_3Cl$ (H_2O): C 60.44, H 7.83, N 3.91, Cl 9.91. Found: C 60.58, H 7.34, N 3.76, Cl 10.02.

2-(1,2,5,6-tetrahydropyridine-N-ethyl)-4-butoxybenzoate N-methyl iodide 10(a) To a solution of 1.00 g of **8a** (0.0033 mol) in 10 mL of acetonitrile, 0.57 g of methyl iodide (0.00395 mol) was added and stirred overnight. The mixture was concentrated and the residue washed with anhydrous ether to promote crystallization. The resulting salt was recrystallized from n-hexanol and vacuum dried to yield 1.037 g (70.45%) of an off-white powder, m.p. 99-100 °C. ^{1}H-NMR (D_2O): δ 7.9 (2H, d), 6.9 (2H, d), 5.9 (1H, m), 5.6 (1H, m), 4.6 (2H, t), 4.0 (2H, t), 3.7 (2H, d), 3.6 (2H, t), 3.5 (2H, t), 3.1 (3H, s), 2.4 (2H, m), 1.6 (2H, m), 1.4 (2H, m), 0.9 (3H, t). Elemental analysis calculated (%) for $C_{19}H_{28}NO_3I$: C 51.24, H 6.34, N 3.15, I 28.50. Found: C 50.80, H 6.18, N 2.92, I 28.72.

2-(1,2,5,6-tetrahydropyridine-N-ethyl)-4-butylbenzoate 8(b). Reagents used: 1.16 g of 4-butyl benzoylchloride (0.0059 mol) dissolved 3 mL of anhydrous ether, 0.75 g of **7** (0.0059 mol) dissolved in 3 mL of anhydrous ether, one gram of sodium carbonate (0.0094 mol). 1.5 g was recovered (89%). Purity was determined by GC-MS. ^{1}H-NMR ($CDCl_3$) δ7.95 (2H, d), 7.3(2H, d), 5.7 (1H, m), 5.65 (1H, m), 4.5 (2H, t), 3.1 (2H, d), 2.9 (2H, t), 2.7 (2H, t), 2.6 (2H, m), 2.2 (2H, t), 1.6 (2H, m), 1.35 (2H, m), 0.9 (3H, t). MS (m/z): M^+ 287.13, 161.12 $[C_{11}H_{13}O]^+$, 109.11 $[C_5H_8N]^+$, 96.06 base $[C_6H_{10}N]^+$, 82.03 $[C_5H_8N]^+$.

2-(1,2,5,6-tetrahydropyridine-N-ethyl)-4-butylbenzoate hydrochloride 9(b) Reagents used: 0.5 g (0.00174mol) of **8b**, hydrogen chloride, 5 mL of acetonitrile. Solid residue was recrystallized from a mixture of n-butanol, carbon tetrachloride and ether to afford 0.402 g (71.4%), mp 115.3-116.5 °C. The sample was first dissolved in just enough warm 1-butanol, carbon tetrachloride was added to double the volume. This mixture was then cooled and anhydrous diethyl ether was added until

solution turned cloudy with white crystals precipitating out with further cooling. ^{1}H-NMR (D_2O): δ7.8 (2H, d), 7.25 (2H, d), 5.85 (1H, m), 5.6 (1H, m), 4.56 (2H, t), 3.8 (2H, t), 3.7 (2H, d), 3.54 (2H, t), 2.55 (2H,t), 2.3 (2H, m), 1.45 (2H, m), 1.15 (2H, m), 0.75 (3H, t). Elemental analysis calculated (%) for $C_{18}H_{26}NO_2Cl$ (H_2O): C 66.76, H 8.09, N 4.33, Cl 10.95. Found: C 66.59, H 7.99, N 4.32, Cl 10.83.

2-(1,2,5,6-tetrahydropyridine-N-ethyl)-4-butylbenzoate N-methyl iodide 10(b) A solution containing 0.86 g (0.0030 mol) of **8(b),** 0.509 g (0.00448 mol) of CH_3I and 5 ml of acetonitrile was stirred at room temperature overnight. The solution was concentrated and solid recrystallized from n-butanol to yield 0.96 g (75 %), mp 110.3-111.6 ^{o}C. ^{1}H-NMR (D_2O) δ7.8 (2H, d), 7.2 (2H, d), 5.9 (1H, m), 5.5 (1H, m), 4.0 (2H, d), 3.8 (2H, m), 3.7 (2H, t), 3.5 (2H, t), 3.1 (3H, s), 2.6 (2H, t), 2.4 (2H, m), 1.5 (2H, m), 1.1 (2H, m), 0.7 (3H, t). Elemental analysis calculated (%) for $C_{19}H_{28}NO_2I$: C 53.15%, H 6.57%, N 3.26%, I 29.56. Found: C 52.85%, H 6.44%, N 3.22%, I 29.63%.

2-(1,2,5,6-tetrahydropyridine-N-ethyl)-4-hexoxybenzoate 8(c) Reagents used: 1.022 g of 4-hexoxy benzoylchloride (0.00425 mol) dissolved 5 mL of anhydrous ether, 0.54 g of **7** (0.00425 mol) dissolved in 5 mL of anhydrous ether, one gram of sodium carbonate (0.0094 mol). 0.94 g of was recovered (67.1%). Purity was determined by GC-MS. ^{1}H-NMR (CD_3COCD_3) δ7.95 (2H, d), 7.05(2H, d), 5.7-5.6 (2H, m), 4.0 (2H, t), 4.1 (2H, t), 3.1 (2H, d), 2.8 (2H, t), 2.7 (2H, t), 2.1 (2H, m), 1.8 (2H, m), 1.5 (2H, m), 1.4 (4H, m), 0.9 (3H, t).MS (m/z): M^+ 331.18, 205.16 $[C_{13}H_{17}O_2]^+$, 109.14 $[C_7H_{11}N]^+$, 96.07 base $[C_6H_{10}N]^+$, 82.02 $[C_5H_8N]^+$.

2-(1,2,5,6-tetrahydropyridine-N-ethyl)-4-hexoxybenzoate hydrochloride 9(c) Hydrogen chloride gas was passed to a solution containing 0.47 g (0.00142 mol) of **8c** in 5 mL of CH_2Cl_2 for one minute. The solution was concentrated and residue recrystallized from n-butanol to afford 0.25 g of 9c (48.0%), m.p. 126-126.5 ^{O}C. ^{1}H-NMR (D_2O) δ7.8 (2H, d), 6.8 (2H, d), 5.9 (1H, m), 5.6 (1H, m), 4.5 (2H, t), 3.9 (2H, t), 3.7 (2H, t), 3.5 (2H, t), 3.4 (2H, t), 2.38 (2H, m), 1.6 (2H, m), 1.35-1.05 (6H, m), 0.75 (3H, t). Elemental analysis calculated (%) for $C_{20}H_{30}NO_3Cl$: C 65.33%, H 8.16%, N 3.80%. Found: C 65.03%, H 8.13%, N 3.77%.

2-(1,2,5,6-tetrahydropyridine-N-ethyl)-4-hexoxybenzoate N-methyl iodide 10(c) A solution containing 0.47 g (0.00142 mol) of **8c,** 1.14 g (0.0074 mol) of CH_3I and 5 ml of acetonitrile was stirred at room temperature overnight. The solution was concentrated and solid residue recrystallized from n-butanol to yield 0.46 g (69 %)**,** mp 107.5-108.5 ^oC. ^1H-NMR (CD_3COCD_3) δ8.1 (2H, d), 7.1 (2H, d), 6.1 (1H, m), 5.9 (1H, m), 4.9 (2H, t), 4.4 (2H, dd), 4.3 (2H, t), 4.0 (2H, t), 3.6 (2H, t), 2.8 (3H, s), 2.7 (2H, m), 2.1 (2H, m), 1.8 (2H, m), 1.5 (2H, m), 1.4 (2H, m), 0.9 (3H, t). Elemental analysis calculated (%) for $C_{21}H_{32}NO_3I$: C 53.31%, H 6.76%, N 2.96%, I 26.82. Found: C 52.88%, H 6.66%, N 2.98%, I 29.87%.

1-(2-hydroxyethyl) piperidine (11) To a mixture containing 10.38 g of piperidine (0.122 mol), 10.818 g of sodium carbonate (0.122 mol) and 50 mL of acetonitrile was added slowly another mixture containing 15.25 g of 2-bromoethanol (0.121 mol) and 50 mL of acetonitrile. The reaction mixture was allowed to stir for 7 additional days at room temperature. The mixture was then concentrated and the residue washed several times with ether. Ether solution was concentrated and residue distilled to afford 5.15 g (33.0%), colorless liquid, bp 59 ^oC/5 mm Hg, n_D 1.4787. MS m/z: M^+ 129.03, 98.06 base $[C_6H_{12}N]^+$, 31 $[CH_2{=}OH]^+$. Literature value: bp 70-75/10 mm Hg, n_D 1.4794. ^1H-NMR (CD_3COCD_3): δ 1.40-1.45 (2H, m), 1.5-1.6 (4H, m), 2.45-2.40 (6H, m), 3.55 (2H, t).

2-(N-Piperidine ethyl) *p*-butylbenzoate 12(b) A solution of 0.50 g (0.0039 mol) of **11** in 5 mL of acetonitrile was added to another mixture containing 0.76 g of 4-butyl benzoyl chloride (0.0039 mol), 0.50 g of sodium carbonate (0.00472 mol) and 5 mL of acetonitrile. After 2 hours of stirring, at room temperature, the sodium carbonate was filtered off and filtrate then made alkaline with 6M sodium hydroxide to pH 8. The mixture was then extracted with ether, dried over magnesium sulfate and concentrated to afford 0.605 g (54%). ^1H-NMR (CD_3COCD_3): δ 7.95 (2H, d), 7.35 (2H, d), 4.4 (2H, t), 2.7 (4H, m), 2.5 (4H, m), 1.65 (2H, m), 1.55 (4H, m), 1.4 (4H, m), 0.9 (3H, t). MS (m/z): M^+ 289, 205.25 $[C_{13}H_{17}O_2]^+$, 98.17 base $[C_6H_{12}N]^+$, 111.17 $[C_7H_{13}N]^+$.

2-(N-Piperidine ethyl) *p*-butylbenzoyl ester N-methyl iodide 13(b) 0.80 mL of iodomethane (0.013 mol) was added to a mixture of 0.30 g of **12b** (0.00104 mol) dissolved in 6 mL of dichloromethane. The solution was allowed to stand overnight at room temperature, concentrated to yield a solid

residue. The solid was then recrystallized from a mixture of n-butanol and ether to yield 0.245 g (54.4%), mp 113.3-114.7 °C. ^{1}H-NMR (D_2O): δ 8.0 (2H, d), 7.4 (2H, d), 4.9 (2H, t), 4.25 (2H, t), 3.9 (4H, t), 2.8 (3H, s), 2.75 (2H, t), 2.1 (6H, m), 1.6 (2H, m), 1.4 (2H, m), 1.0 (3H, t). Elemental analysis calculated (%) $C_{19}H_{30}NO_2I$: C 52.93, H 6.96, N 3.25, I 29.44. Found: C 52.67, H 7.14, N 3.18, I 30.17.

2-(N-Piperidine ethyl) *p*-tertbutylbenzoate 12(c) A solution of 0.50 g (0.0039 mol) of **11** in 5 mL of acetonitrile was added to another mixture containing 0.76 g of 4-tertbutyl benzoyl chloride (0.0039 mol), 0.50 g of sodium carbonate (0.00472 mol) and 5 mL of acetonitrile. After 2 hours of stirring, at room temperature, the sodium carbonate was filtered off and filtrate then made alkaline with 6M sodium hydroxide to pH 8. The mixture was then extracted with ether, dried over magnesium sulfate and concentrated to afford 0.67 g (60%). ^{1}H-NMR (CD_3COCD_3): δ 7.95 (2H, d), 7.6 (2H, d), 4.4 (2H, t), 2.75 (2H, t), 2.5 (4H, t), 1.6 (6H, m), 1.4 (9H, s).

2-(N-Piperidine ethyl) *p*-tertbutylbenzoyl ester N-methyl iodide 13(c) same procedure as in **13b** with 0.305 gram (0.00106 mol) of **12c** in 5 ml of CH_2Cl_2 to afford 0.21 g of **13c** (46%) after recrystallization from n-butanol, m.p. 152.8-154.2 °C. ^{1}H-NMR (D_2O): δ 7.82 (2H, d), 7.5 (2H, d), 4.7 (2H, t), 3.75 (2H, t), 3.5-3.3 (4H, t), 3.1 (3H, s), 1.9-1.7 (4H, m), 1.4-1.35 (2H, m), 1.1 (9H, s). Elemental analysis calculated (%) for $C_{19}H_{30}NO_2I$: C 52.90, H 6.96, N 3.24. Found: C 52.48, H 7.07, N 3.12.

2-(N-Piperidine ethyl) *p*-butylbenzoyl ester N-methyl iodide 14(b) HCl gas was passed through a mixture of 0.30 g of **12b** (0.001014 mol) for several minutes. The solution was concentrated to afford 0.39 g of a solid residue. The solid was then recrystallized from a mixture of n-butanol and ether to yield 0.136 g (40.0%), mp 159.6-160.8 °C. ^{1}H-NMR (D_2O): δ 7.8 (2H, d), 7.3 (2H, d), 4.5 (2H, t), 3.5 (4H, m), 3.0 (2H, bm), 2.6 (2H, t), 2.75 (2H, t), 1.8-1.6 (6H, m), 1.45 (2H, m), 1.2 (2H, m), 0.75 (3H, t). Elemental analysis calculated (%) for $C_{18}H_{28}NO_2Cl$: C 66.39, H 8.60, N 4.30, Cl 10.89. Found: C 66.24, H 8.36, N 4.33, Cl 10.74.

Cell Culture and Membrane Preparation

Chinese hamster ovary cells stably transfected with the genes of human variants of muscarinic receptors and cDNA coding G_{15} G-protein were purchased from Missouri S&T cDNA Resource Center (Rolla, MO, USA). M_2 or M_4 receptors were connected to phospholipase C pathway by G_{15} G-protein that was cotransfected into CHO cells. [26] Stable cell lines were established by selection of hygromycine B resistant clones. Cell cultures and crude membranes were prepared as described previously. [27] Cells were grown to confluence in 75 cm^2 flasks in Dulbecco's modified Eagle's medium supplemented with 10% fetal bovine serum and 2 million of cells were sub-cultured to 100 mm Petri dishes. Medium was supplemented with 5 mM butyrate for the last 24 hours of cultivation to increase receptor expression. Cells were detached by mild trypsinization on day 5 after subculture. Detached cells were washed twice in 50 ml of phosphate-buffered saline and 3 min centrifugation at 250 × g. Washed cells were suspended in 20 ml of ice-cold incubation medium (100 mM NaCl, 20 mM Na-HEPES, 10 mM $MgCl_2$, pH = 7.4) supplemented with 10 mM EDTA and homogenized on ice by two 30 s strokes using Polytron homogenizer (Ultra-Turrax; Janke & Kunkel GmbH & Co. KG, IKA-Labortechnik, Staufen, Germany) with a 30 s pause between strokes. Cell homogenates were centrifuged for 30 min at 30,000 × g. Supernatants were discarded, pellets suspended in fresh incubation medium, incubated on ice for 30 minutes and centrifuged again. Resulting membrane pellets were kept at - 80 °C until assayed within 10 weeks at a maximum.

Radioligand Binding Experiments

All radioligand binding experiments were optimized and carried out as described earlier. Briefly, membranes were incubated in 96-well plates at 30 °C in the incubation medium described above. Incubation volume was 400 µl or 800 µl for competition and saturation experiments with [^{3}H]NMS, respectively. Approximately 30 µg of membrane proteins per sample were used. N-methylscopolamine binding was measured directly in saturation experiments using six concentrations (30 pM to 1000 pM) of [^{3}H]NMS for 1 hour. For calculations of equilibrium

dissociation constant (K_D), concentrations of free [^{3}H]NMS were calculated by subtraction of bound radioactivity from total radioactivity in the sample and fitting equation 1 (**data analysis section**). Binding of tested ligands was determined in competition experiments with 1 nM [^{3}H]NMS and inhibition constant K_I was calculated according Eq. 3. Nonspecific binding was determined in the presence of 1 μM unlabeled atropine. Incubations were terminated by filtration through Whatman GF/C glass fiber filters (Whatman) using a Brandel cell harvester (Brandel, Geithesburg, MD, USA). In kinetic experiments membranes were pre-incubated with 1nM [^{3}H]NMS for 1 hour (M_2), 3 hours (M_1, M_3, M_4) or 5 hours (M_5). Then dissociation was started by addition of atropine to final concentration of 10 μM. Atropine was added either alone or in mixture with antagonist at final concentration of 100 μM. Dissociation was terminated by filtration after 5 min (M_2), 30 min (M_1, M_3), 40 min (M_4) or 2 hours (M_5) Filters were dried in microwave oven and then solid scintillator Meltilex A was melted on filters (105 °C, 90 s) using a hot plate. The filters were cooled and counted in Wallac Microbeta scintillation counter.

Accumulation of Inositol phosphates

Accumulation of inositol phosphates was measured according to Michal et al. [28] Inositolphosphates formation was determined in cells pre-labeled overnight by 0.5 μM [^{3}H]myo-inositol in 0.3 ml of DMEM (3 μCi/ml) at 37 °C. Cells were then washed with fresh medium and pre-incubated in 0.4 ml of DMEM containing 10 mM LiCl and ± tested compound for 15 min at 37°C. Then agonist carbachol was added and samples were incubated for additional 20 min in final volume 0.5 ml. Incubation was stopped by removal of incubation buffer and addition 0.2 ml 20% trichloracetic acid (TCA). After 1 h incubation at 4 °C, 100 μl of TCA extracts were taken for measurement. Rest of the TCA was removed, and TCA precipitates were washed with 200 μl TCA and dissolved in 300 μl of 1 M NaOH. After 1 h incubation at 4 °C, 100 μl of NaOH lysates were taken for measurement. Radioactivity in TCA extracts and NaOH lysates were determined by liquid scintillation counting. The rate of inositolphosphates accumulation was calculated as a percentage of the soluble (released) inositolphosphates from the total incorporated radioactivity (sum of radioactivity in NaOH lysates and TCA extracts).

Binding and activation parameters of CHO cells

Equilibrium dissociation constants (K_D) and maximum binding capacities (B_{MAX}) of [^{3}H]NMS were obtained by fitting Equation 1 (**data analysis section**) to the data from saturation binding experiments (**table 1**). K_D values are expressed as negative logarithms and B_{MAX} values as pmol of binding sites per mg of membrane protein. Inhibition constants Ki of carbachol were calculated according equation 3 (**data analysis section**) and are expressed as negative logarithms. % low denotes percentage of low affinity binding sites for carbachol. Half-efficient concentrations (EC_{50}) and maximal effects (E_{MAX}) of carbachol were obtained by fitting equation 4 (**data analysis section**) to the data from measurements of accumulation of inositol phosphates. EC_{50} values are expressed as negative logarithms and E_{MAX} values as folds over basal. Values are means ± SD.

Determination of Acetylcholinesterase Activity

Acetylcholinestarase activity in samples (**figure 1**) mimicking binding and functional or assay conditions was determined by decrease in recovery of ^{14}C-acetylcholine in organic phase of tetraphenyl borate precipitation assay. [29] Acetylcholine radiolabeled by ^{14}C in the acetate was added to either wells containing only buffer or also washed adherent cells or cell membranes to final concentration of 50 nM. After 20 min incubation at 37 ºC (adherent cells) or 3 hours at 30 ºC (membranes), membranes were spin down, supernatant was taken out and combined 1:1 with sodium tetraborate in 3-heptanone (15 mg/ml). Samples were vigorously vortexed, centrifuged 15 min at 3,000 × g to separate the organic and aqueous phases. Aliquots of the organic phase were taken for scintillation counting.

Data analysis

Data from biological evaluation experiments were processed in Libre Office, analyzed and plotted using program Grace. [30] Statistical analysis was performed using statistical package R. [31] For non-linear regression analysis following equations were used:

[^{3}H]NMS saturation binding

$$y = \frac{B_{MAX} * x}{x + K_D} \qquad \text{Eq. 1}$$

where y is specific binding at free concentration x, B_{MAX} is maximum binding capacity, and K_D is equilibrium dissociation constant.

Competition binding

$$y = 100 - \frac{100 * x}{x + IC_{50}} \qquad \text{Eq. 2}$$

where y is specific radioligand biding at concentration x of competitor expressed as percent of binding in the absence of competitor, IC_{50} is concentration causing 50 % inhibition of radioligand binding. Inhibition constant K_I was calculated as:

$$K_I = \frac{IC_{50}}{1 + \frac{[D]}{K_D}} \qquad \text{Eq. 3}$$

where IC_{50} is concentration causing 50 % inhibition of [^{3}H]NMS binding calculated according Eq. 2 from competition binding data, [D] is concentration of [^{3}H]NMS used, and K_D is its equilibrium dissociation constant calculated according Eq. 1 from saturation binding data. [32]

Concentration response

$$y = 1 + \frac{(E_{MAX} - 1) * x^{nH}}{x^{nH} + EC_{50}} \qquad \text{Eq. 4}$$

where y is response normalized to basal (in the absence of carbachol) at ligand concentration x, E_{MAX} is maximal effect, EC_{50} is concentration causing half-maximal effect, and nH is Hill coefficient.

Equilibrium dissociation constant of antagonism of functional response K_B was calculated from the shift in EC_{50} of functional response to carbachol by antagonist according Eq. 5 (determination from a single antagonist concentration) or Eq. 6 (determination from six concentration of antagonist)

$$\log(DR-1) = \log(K_B) - \log([B]) \quad \text{Eq. 5}$$

$$\log(DR-1) = \log\left[\frac{[B](1-\alpha)}{\alpha[B]+K_B}\right] \quad \text{Eq. 6}$$

where DR is ratio of EC_{50} of the functional response in the presence to the absence of antagonist B and α is a factor of cooperativity between carbachol and antagonist.

RESULTS

Synthesis

Compound **6** (**scheme 1)** was synthesized by reacting pyridine with 2-bromoethanol and then selectively reduced with sodium borohydride to produce compound **7**. [24] Reaction of **7** with p-substituted benzoyl chlorides afforded compounds **8a-c** which were then treated with hydrogen chloride gas and iodomethane to afford salts **9a-c** and **10a-c**, respectively.

Compound **11** (**scheme 2**) was formed by reacting piperidine with 2-bromoethanol and then treated with several p-substituted benzoyl chlorides to yield compounds **12a-c**. Compounds **12a-c** reacted with iodomethane and hydrogen chloride to produce the corresponding salts **13a-c** and **14a-b**, respectively.

Biological Evaluation

Affinity of compounds (**schemes 1 & 2**) was assessed in competition experiments with 1 nM [^{3}H]NMS. All tested compounds completely inhibited [^{3}H]NMS binding. Inhibition constants K_I (expressed as pK_I), calculated according to equation 3 (**data analysis section**), micromolar range, are summarized in **table 2**.

Our novel ligands (**9a-14b**) bind to all receptor subtypes and display the same affinity for all receptors with some exceptions. Compound **13a** displays slightly (three to eight fold) higher affinity for M_2 receptor, **9b** displays slightly (two to three-fold) higher affinity for M_1 receptor, **14b** displays slightly (two to five fold) higher affinity for the M_2 receptor, **9a**, **13(b-c)** display slightly (two to four fold) higher affinity for the M_2 receptor, **9c** displays slightly (1 to 3 fold) for M_2 receptor, and compound **10c** displays slightly higher affinity (one to three fold) for the M_2 and M_5 receptors. In general, analogs with a quaternary ammonium group bind with higher affinity than those with a tertiary cationic group at all receptor subtypes with the exception of **13c** with R= tert-C_4H_9. Thus potency of **10b > 9b**, **10a > 9a**, and **13b > 14b> 13c**. Furthermore, compound **10c** with a para-substituted O-n-C_6H_{13} group displays appreciably higher affinity than other compounds at all receptors.

Ability of tested compounds to antagonize functional response at muscarinic receptors was determined in measurements of carbachol induced accumulation of inositol phosphates. Antagonism of tested compounds was determined at single high concentration of 0.1 mM. All tested compounds antagonized functional response to carbachol and increased carbachol half-efficient concentration (EC_{50}). Based on shift in the EC_{50} by antagonist equilibrium dissociation constants (K_B) of antagonists were calculated according equation 5 (**data analysis section**) and are summarized in **table 3**. The most potent antagonist among tested compounds was **10c** displaying K_B in nanomolar range, with exception of M_2 receptor.

A full Schild regression analysis (**figure 2**) for representative antagonist **10a** was performed with pK_B and alpha (α) values shown in **table 4.**

All Compounds slowed down in [^{3}H]NMS dissociation as summarized in **table 5** and **figure 3.** The existence of the secondary binding site is supported by slow-down in [^{3}H]NMS dissociation as any change of the ligand kinetic is conditioned by concurrent binding of two ligands to the receptor and concurrent binding of two ligands may occur only to two distinct sites.

Acetylcholinestarase activity in samples (**figure 1**) mimicking binding and functional or assay conditions was determined by decrease in recovery of ^{14}C-acetylcholine in organic phase of tetraphenyl borate precipitation assay.

DISCUSSION

The major finding of this pilot study is the identification of M_1/M_4 functionally selective muscarinic antagonists structurally related to agonist AC-42. All five muscarinic receptor subtypes share high sequence homology, especially in the orthosteric binding site. Current crystallographic structures of M_2 and M_3 receptors show that homology in the secondary and tertiary structure extends even beyond the orthosteric binding site.[25] This high homology hinders the discovery of ligands that bind selectively to specific receptor subtypes. This study describes various functionally selective ligands (ligands that preferentially activate only some receptor subtypes or signaling pathways) that bind to all receptor subtypes with the same affinity. Functionally selective ligands thus appear to be possible way for selective modulation of function of muscarinic receptors.

Complete inhibition of the orthosteric antagonist [^{3}H]NMS suggests steric interaction (mutual exclusivity of binding) between tested compounds and [^{3}H]NMS. On the other hand, in some cases, antagonism of carbachol induced functional response by compounds suggests non-competitive interaction between compounds and carbachol as potency of functional antagonism (pK_B) is greater than affinity of the compounds (pK_I) (**table 3 versus table 2**). A full Schild regression analysis of representative compound **10a** shows inhibition of carbachol response is indeed allosteric with factor cooperativity alpha (α) of about 0.001 (potency limits to about 1000-fold decrease) and K_B values about 2-fold underestimated, so the difference between K_B and K_i is even greater (**table 4, figure 2**). This discrepancy is explained by existence of the secondary binding site to which new compounds bind with higher affinity than to the orthosteric binding site. From this secondary site, these compounds block receptor activation but do not inhibit [^{3}H]NMS binding. The existence of the secondary binding site is supported by slow-down in [^{3}H]NMS dissociation (**table 5, figure 3**) as any

change of the ligand kinetic is conditioned by concurrent binding of two ligands to the receptor and concurrent binding of two ligands may occur only to two distinct sites.

Interestingly, compounds **9b**, **10a** and **10b** are much more potent antagonists at M_1 and M_4 receptors than at the rest of subtypes. These compounds are considered M_1/M_4 functionally selective antagonists. The most potent antagonist among tested compounds was **10c** displaying K_B in nanomolar range with exception of M_2 receptor (**table 3**). These novel prototypical compounds of functionally selective M_1/M_4 antagonists may provide a viable approach for the treatment of certain central nervous system disorders including Parkinson disease (PD).

Finally, acetylcholinestarase activity in samples (**figure 1**) mimicking binding and functional or assay conditions was determined by decrease in recovery of ^{14}C-acetylcholine in organic phase of tetraphenyl borate precipitation assay. Recovery of [^{14}C] acetylcholine in the organic phase is the same under all experimental conditions suggesting that no detectable acetylcholinesterase activity in the samples.

ACKNOWLEGMENTS

This work was supported by the Academy of Sciences of the Czech Republic support [RVO:67985823], the Grant Agency of the Czech Republic grants [14-05696S] and [P304/12/G069] and by the Department of Physical Sciences at Barry University.

FIGURE LEGENDS

Scheme 1. Synthesis of N-Substituted 4-Benzoyl Tetrahydropyridinyl Salts

Scheme 2. Synthesis of N-Substituted p-Benzoyl Piperidinyl Salts

Table 1. Equilibrium dissociation constants (K_D) and maximum binding capacities (B_{MAX}) of [^{3}H]NMS

Table 2. Binding equilibrium constants (expressed as pK_I) calculated from equation 3 and expressed as negative logarithms. (*) Higher than at other subtypes ($p<0.05$, ANOVA, Dunnet's post-test), values are means ± SD.

Table 3. Equilibrium dissociation constants of antagonist competition of functional response to carbachol. Equilibrium dissociation constants K_B obtained by fitting Eq. 5 to the data from functional response assays in the presence of antagonist and expressed as negative logarithms. (*) Greater than inhibition constant pK_i in table 2 ($p<0.05$, t-test).

Table 4. Equilibrium dissociation constants of compound **10a** competition of functional response to carbachol. Equilibrium dissociation constants K_B and factors of cooperativity obtained by fitting Eq. 6 to the data from functional response assays in the presence of antagonist. K_B values expressed as negative logarithms. Data are means ± SD from 3 independent experiments performed in triplicates. (*) Different from other subtypes ($p<0.05$, ANOVA, Tukey HSD post-test).

Table 5. Rate dissociation constants k_{off} of [^{3}H]NMS dissociation in the absence (control) or presence of competitor in the final concentration of 0.1 mM expressed in min^{-1}. (*) Different from control ($p<0.05$, t-test), values are means ± SD.

Figure 1. Acetylcholineterase Activity. [^{14}C] acetylcholine recovery in the organic phase expressed as percent of added radioactivity. Values are means ± SD from 3 independent experiments performed in duplicates.

Figure 2. Schild regression analysis of compound **10a** antagonism. Logarithms of dose ratios (DR) of inositol phosphates accumulation induced by carbachol in the presence to absence of compound **10a** at individual subtypes of muscarinic receptors plotted against used concentration of **10a**. Data are means ± SD from 3 independent experiments preformed in triplicates.

Figure 3. Effect of antagonists on [^{3}H]NMS dissociation. Membranes incubated with 1nM [^{3}H]NMS for 1 hour (M_2), 3 hours (M_1, M_3, M_4) or 5 hours (M_5). Dissociation started by addition of atropine to final concentration of 10 μM. Atropine added either alone or in mixture with antagonist at final concentration of 100 μM. Dissociation terminated by filtration after 5 min (M_2), 30 min (M_1, M_3), 40 min (M_4) or 2 hours (M_5). Data are means ± SD from 3 independent experiments preformed in quadruplicates.

CONFLICT OF INTEREST

I have no conflict of interest

REFERENCES

[1] A. Fisher,. Neurodegener. Dis. **2008**, 5, 237–240.

[2] C. Langmead, J. Watson, C. Reavill, Pharmacol. Ther. **2008**, 117, 232–243.

[3] D. Dencker, M. Thompson, G. Wortwein, P. Welkop, Y. Cui, J. Jeon, J. Wess, A. Fink-Jensen, ACS Chem. Neurosc. **2012**, 3, 2, 80-89.

[4] N. Mirza, D. Peters, R. Sparks, CNS Drug Rev. **2003**, 9, 159–186.

[5] F. Bymaster, C. Whitesitt, H. Shannon, N. DeLapp, J. Ward, D. Calligaro, L. Shipley, J. Buelke-Sam, N. Bodick, L. Farde, M. Sheardown, P. Olesen, K. Hansen, P. Suzdak, M. Swedberg, P. Sauerberg, C. Mitch, Drug Dev. Res. **1997**, 40, 158–170.

[6] N. Bodick, W. Offen, A. Levey, N. Cutler, S. Gauthier, A. Satlin, H. Shannon, G. Tollefson, K. Rasmussen, F. Bymaster, D. Hurley, W. Potter, S. Paul, Arch. Neurol. **1997**, 54, 465–473.

[7] A. Korczyn, Expert Opin. Invest. Drug. **2000**, 9, 2259–2267.

[8] C. Langmead, A. Christopoulos, Trends Pharmacol. Sci. **2006**, 27, 475–481.

[9] J. Wess, Mol. Pharmacol. **2005**, 68, 1506–1509.

[10] S. Lazareno, A. Popham, N. Birdsall, Mol.Pharmacol. **2000**, 58, 194–207.

[11] L. Ma, M. Seager, M. Wittman, M. Jacobson, D. Bickel, M. Burno, K. Jones, V. Graufelds, G. Xu, M. Pearson, A. McCampbell, R. Gaspar, P. Shughrue, A. Danziger, C. Regan, R. Flick, D. Pascarella, S. Garson, S. Doran, C. Kreatsoulas, L. Veng, C. Lindsley, W. Shipe, S. Kuduk, C. Sur, G. Kinney, G. Seabrook, W. Ray, Proc. Natl. Acad. Sci. U.S.A. **2009**, 106, 15950–15955.

[12] A. Christopoulos, R. Dror, Nature**, 2013**, 000, 1-5.

[13] K. Haga, Nature, **2012**, 482, 547–551.

[14] W. Liu, Science, **2012**, 6091, 232–236 .

[15] S. Rasmussen, Nature, **2011**, 477, 549–555.

[16] C. Valant, P. Sexton, A. Christopoulos, Mol. Interventions, **2009**, 9, 125−135.

[17] J. Lane, P. Sexton, A. Christopoulos, Trends in Pharm. Sci. **2013**, 34, 1, 59-66

[18] M. Grant, E. El-Fakahany, JPET **2005**, 153, 313-319.

[19] V. Avlani, C. Langmead, E. Guida, M. Wood, B. Tehan, H. Herdon, J. Watson, Sexton, A. Christopoulos, Mol. Pharmacol. **2010**, 78, 94−104.

[20] J. Boulos, J. Jakubik, A. Randakova, H. Dao, J. Heter. Chem. **2013**, 50, 6, 1363-1367.

[21] Z. Xiang, A. Thompson, C. Jones, C. Lindsley, P. Conn, J. Pharmacol. Exp. Ther. **2012,** 340, 3, 595-603.

[22] D. Sheffler, R. Williams, T. Bridges, Z. Xiang, A. Kane, N. Byun, S. Jadhav, M. Mock, F. Zheng, M. Lewis, C. Jones, C. Niswender, C. Weaver, C. Lindsley, J. Conn, Mol. Pharmacol. **2009**, 76, 356-368.

[23] J. Jeon, D. Dencker, G. Wortwein, D. Woldbye, Y. Cui, A. Davis, A. Levey, G. Schutz, T. Sager, A. Mork, C. Li, C. Deng, A. Fink-Jensen, J. Wess, J. Neurosci. **2010**, 30, 6, 2396-2405.

[24] Y. Niu, L. Wen, A. Chen, X. Lei, Chin. J. Pharm. **2003**, 34, 11, 541-578.

[25] A. Kruse, J. Hu, A. Pan, D. Arlow, A. Rosesenbaum, E. Rosemond, H. Green, T. Liu, P. Chae, R. Dror, D. Shaw, W. Weis, J. Wess, B. Kobilka, Letter, **2012***,* 482, 552-559.

[26] G. Milligan, F. Marshall, S. Rees, Trends Pharmacol Sci. **1996**, 17**,** 235-237.

[27] J. Jakubik, E. El-Fakahany, V. Dolezal, Mol. Pharmacol. **2006**, 70, 656-666.

[28] P. Michal, V. Rudajev, E. El-Fakahany, V. Dolezal, Eur. J. Pharmacol. **2009**, 606, 50-60.

[29] S. Tucek, J. Physiol. **1982**, 322, 53-69.

[30] Grace Development Team Grace: A plotting tool. **2014**, http://hplasma-gate.weizmann.ac.il/Grace/

[31] R Core Team: A Language and Environment for Statistical Computing. *R Foundation for Statistical Computing*, Vienna, Austria. **2014**, http://www.R-project.org

[32] Y. Cheng, W. Prusoff, Biochem. Pharmacol. **1973**, 22, 3099-3108.

Table 1.

	[^{3}H]NMS		Carbachol				
	pK_D	B_{MAX}	pK_{ihigh}	pK_{ilow}	% low	pEC_{50}	E_{MAX}
M_1	9.60 ± 0.04	1.8 ± 0.2	7.71 ± 0.07	4.73 ± 0.05	87 ± 8	5.7 ± 0.1	3.6 ± 0.2
M_2	9.43 ± 0.05	1.3 ± 0.2	7.88 ± 0.05	4.78 ± 0.05	63 ± 5	5.6 ± 0.1	2.9 ± 0.2
M_3	9.64 ± 0.04	1.7 ± 0.2	7.79 ± 0.07	4.74 ± 0.05	85 ± 8	5.9 ± 0.1	3.1 ± 0.2
M_4	9.66 ± 0.05	0.9 ± 0.1	7.85 ± 0.05	4.77 ± 0.05	66 ± 5	5.4 ± 0.1	2.8 ± 0.2
M_5	9.52 ± 0.05	1.0 ± 0.1	7.82 ± 0.07	4.76 ± 0.05	82 ± 8	5.7 ± 0.1	2.5 ± 0.2

Table 2.

Compounds	M_1	M_2	M_3	M_4	M_5
9a	5.2 ± 0.02	5.5 ± 0.1*	5.1 ± 0.04	4.9 ± 0.1	5.2 ± 0.04
9b	5.1 ± 0.1*	4.7 ± 0.05	4.8 ± 0.1	4.6 ± 0.1	4.6 ± 0.2
9c	5.37 ± 0.04	5.5 ± 0.1	5.2 ± 0.2	5.0 ± 0.1	5.2 ± 0.1
10a	5.7 ± 0.2	5.7 ± 0.2	5.2 ± 0.1	5.1 ± 0.1	5.5 ± 0.2
10b	5.6 ± 0.1	5.6 ± 0.2	5.4 ± 0.1	5.4 ± 0.1	5.8 ± 0.1
10c	6.5 ± 0.1	6.8 ± 0.1	6.4 ± 0.1	6.4 ± 0.1	6.8 ± 0.1
13a	5.5 ± 0.02	6.04 ± 0.01*	5.5 ± 0.01	5.12 ± 0.02	5.54 ± 0.05
13b	5.5 ± 0.1	6.0 ± 0.1*	5.69 ± 0.03	5.4 ± 0.1	5.61 ± 0.05
13c	5.08 ± 0.06	5.4 ± 0.1*	5.0 ± 0.1	4.87 ± 0.02	4.85 ± 0.04
14b	5.4 ± 0.1	5.7 ± 0.2	5.2 ± 0.04	5.01 ± 0.05	5.3 ± 0.2

Table 3.

Compounds	M_1	M_2	M_3	M_4	M_5
9a	4.0 ± 0.2	4.6 ± 0.1	4.2 ± 0.1	3.8 ± 0.1	4.4 ± 0.2
9b	7.03 ± 0.03*	4.63 ± 0.05	5.10 ± 0.09*	6.28 ± 0.08*	5.4 ± 0.1*
9c	7.22 ± 0.09*	5.47 ± 0.08*	6.3 ± 0.1*	5.42 ± 0.09*	5.65 ± 0.05*
10a	7.03 ± 0.03*	5.5 ± 0.1	5.19 ± 0.03	6.3 ± 0.1*	5.5 ± 0.1
10b	7.08 ± 0.04*	5.4 ± 0.1	5.5 ± 0.1	6.3 ± 0.1*	5.7 ± 0.1
10c	7.31 ± 0.03*	5.4 ± 0.1	7.10 ± 0.02*	6.4 ± 0.1*	7.03 ± 0.04*
13a	5.49 ± 0.05	5.70 ± 0.02	5.4 ± 0.1	5.3 ± 0.1*	5.1 ± 0.1
13b	6.91 ± 0.02*	5.31 ± 0.05	5.84 ± 0.05*	5.3 ± 0.1	6.14 ± 0.04*
13c	5.93 ± 0.05*	5.21 ± 0.03	5.41 ± 0.06*	5.43 ± 0.03*	5.3 ± 0.1*
14b	6.67 ± 0.04*	5.41 ± 0.05	6.10 ± 0.02*	5.34 ± 0.1*	5.85 ± 0.04*

Table 4.

	pK_B	α
M_1	7.41 ± 0.04*	0.0010 ± 0.0002
M_2	5.81 ± 0.03	0.0014 ± 0.0002
M_3	5.50 ± 0.02	0.0013 ± 0.0002
M_4	6.59 ± 0.03*	0.0012 ± 0.0002
M_5	5.79 ± 0.03	0.0009 ± 0.0002

Table 5.

	M_1	M_2	M_3	M_4	M_5
Control	0.055 ± 0.002	0.262 ± 0.001	0.044 ± 0.002	0.060 ± 0.001	0.0242 ± 0.0004
9a	0.037 ± 0.002*	0.15 ± 0.01*	0.036 ± 0.002*	0.043 ± 0.001*	0.0142 ± 0.0003*
9b	0.045 ± 0.001*	0.194 ± 0.005*	0.035 ± 0.001*	0.045 ± 0.002*	0.0174 ± 0.0002*
9c	0.035 ± 0.002*	0.157 ± 0.005*	0.035 ± 0.002*	0.043 ± 0.003*	0.0141 ± 0.0003*
10a	0.039 ± 0.001*	0.164 ± 0.002*	0.040 ± 0.001*	0.044 ± 0.001*	0.0160 ± 0.0006*
10b	0.046 ± 0.002*	0.15 ± 0.01*	0.036 ± 0.001*	0.039 ± 0.001*	0.0152 ± 0.0002*
10c	0.035 ± 0.001*	0.14 ± 0.01*	0.032 ± 0.001*	0.036 ± 0.001*	0.0142 ± 0.0002*
13a	0.042 ± 0.002*	0.15 ± 0.01*	0.036 ± 0.002*	0.043 ± 0.002*	0.0159 ± 0.0005*
13b	0.044 ± 0.002*	0.15 ± 0.01*	0.036 ± 0.002*	0.033 ± 0.002*	0.0155 ± 0.0003*
13c	0.042 ± 0.003*	0.16 ± 0.01*	0.040 ± 0.002*	0.044 ± 0.001*	0.0169 ± 0.0006*
14b	0.044 ± 0.001*	0.16 ± 0.01*	0.034 ± 0.003*	0.035 ± 0.002*	0.0152 ± 0.0007*

Figure 1.

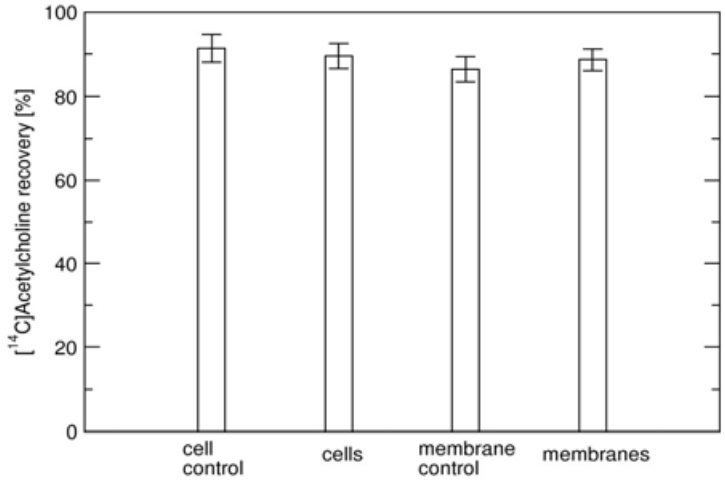

Figure 2.

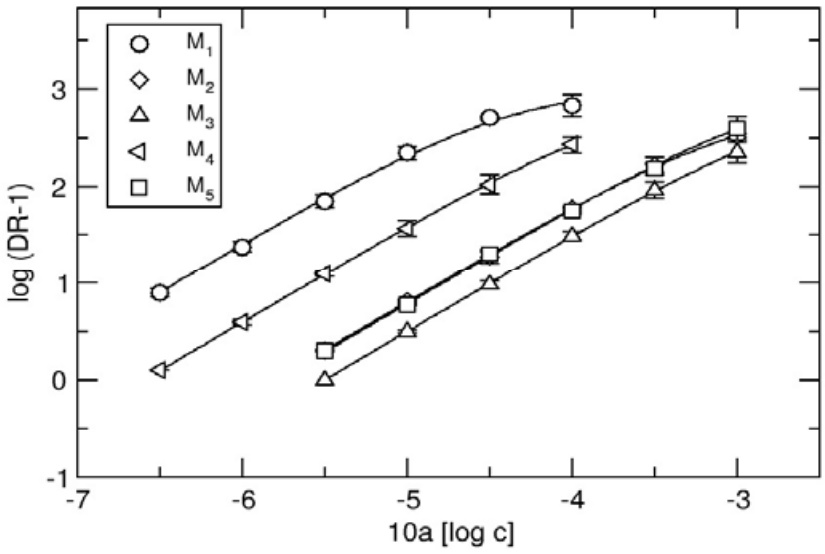

Figure 3.

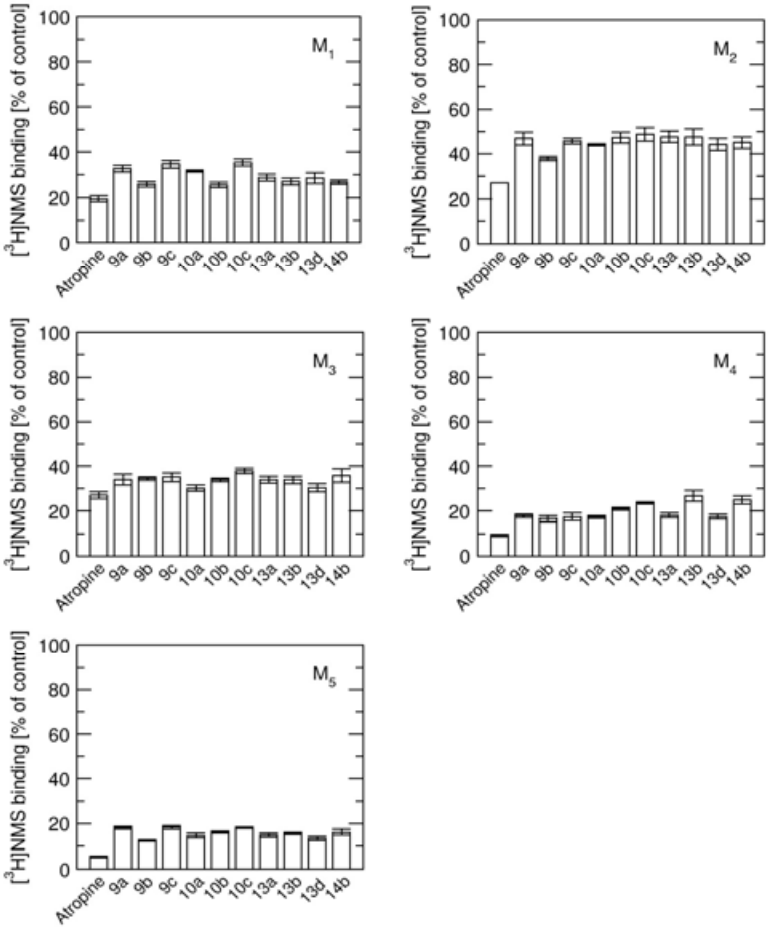

Scheme 1.

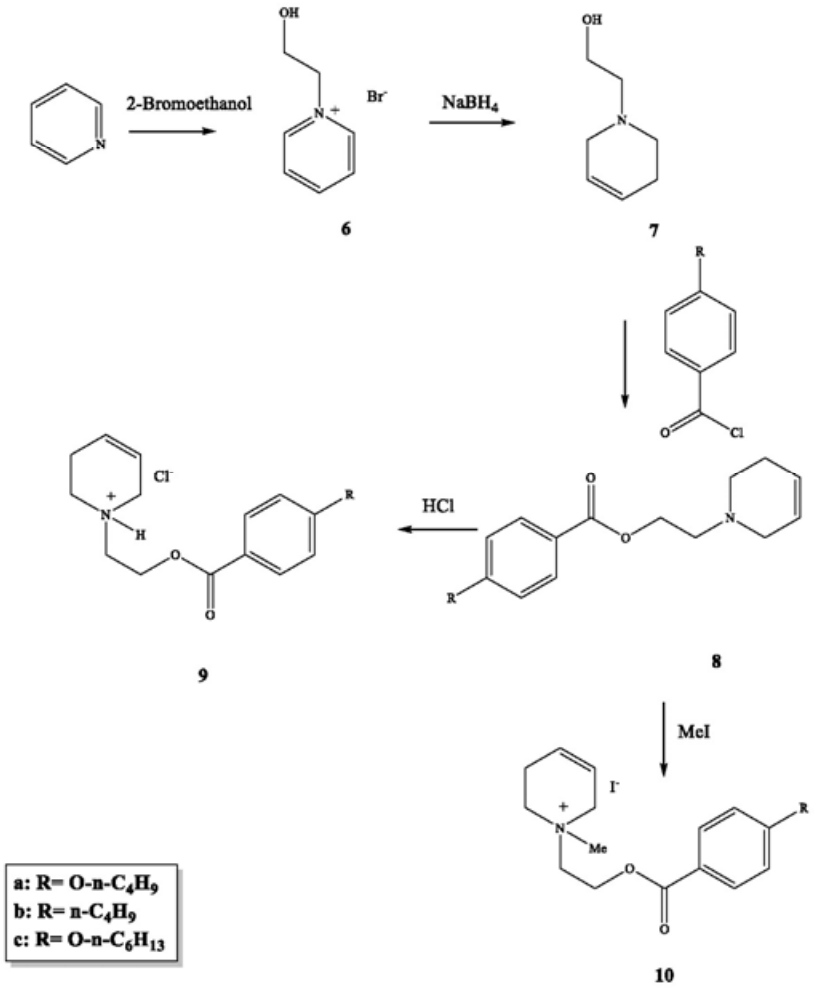

6 7 8 9 10

Scheme 2.

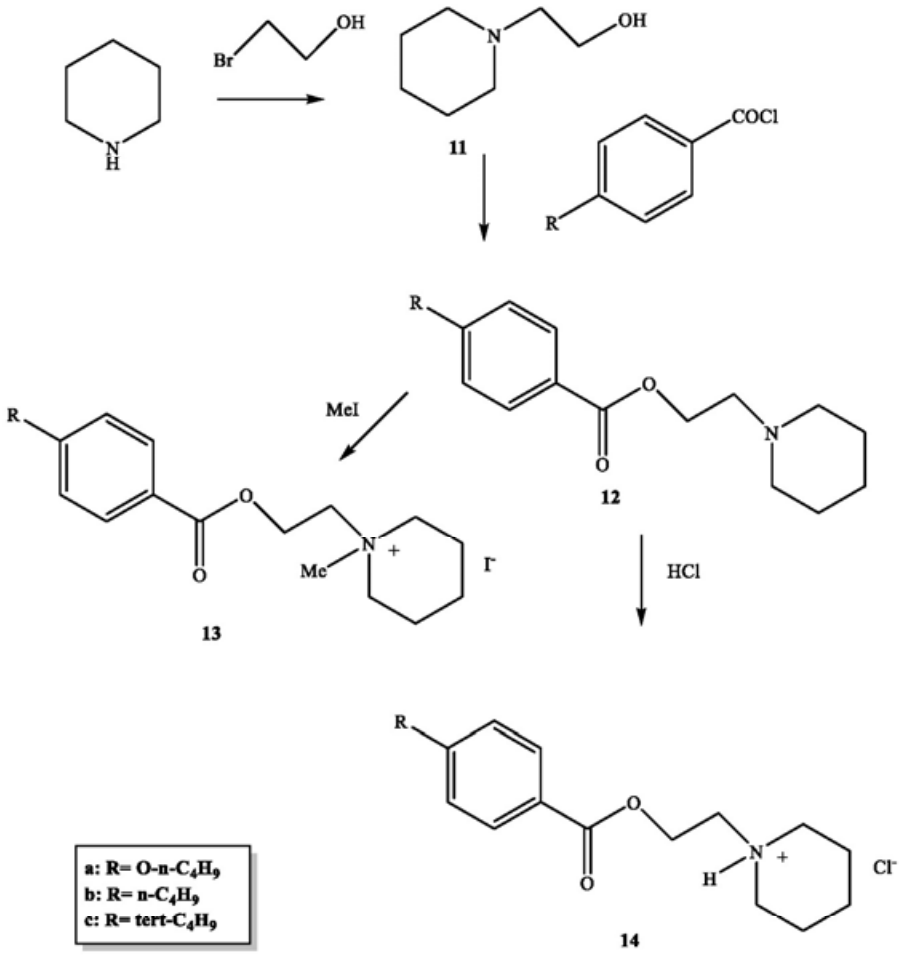

Structure 1.

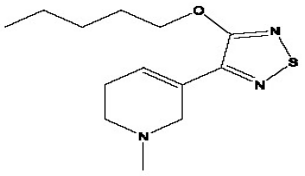

(1)

Structure 2.

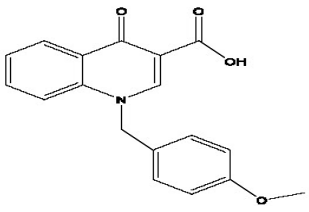

(2)

Structure 3.

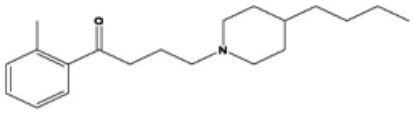

(3)

Structure 4.

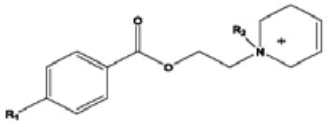

(4)

Structure 5.

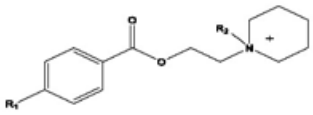

(5)